01 Sep 1975

Measurement of the Low-Wavenumber Component of Turbulent Boundary Layer Pressure Spectral Density

P. W. Jameson

MEASUREMENT OF THE LOW-WAVENUMBER COMPONENT OF TURBULENT BOUNDARY LAYER PRESSURE SPECTRAL DENSITY

Paul W. Jameson
Bolt Beranek and Newman Inc.
Cambridge, Massachusetts 02138

ABSTRACT

This paper describes an experiment in which the turbulent boundary layer (TBL) over a flat plate excites bending waves in that plate predominantly through low-wavenumber components in the pressure field having the same wavenumber as the bending waves of the plate. The plate design is such that contributions to the bending waves from the convective peak of the TBL pressure and from acoustic noise are minimal. The level of response of individual modes of the plate is used to measure the intensity of these low-wavenumber spectral components in the TBL wall pressure.

INTRODUCTION

There is interest in the low-wavenumber region of the turbulent boundary layer (TBL) wall-pressure spectrum, because pressure spectral components at an appropriately low wavenumber are capable of resonant interaction with the natural waves of typical naval structures. These pressure components, then, cause a vibrational floor for a structure moving through the water.

Blake and Chase (1969) and Jameson (1970) employed a phased array of four condenser microphones to measure this low-wavenumber region in a wind-tunnel flow. Jameson's experiment showed that the low-wavenumber spectral density was very low — so low that, in the experiment, the presumed contribution to the measured results were only about 5 dB above the estimated contribution from the convective peak. The experiment was then redone to reduce the contaminating contributions from the convective peak, the modes of a damped plate being used to measure the TBL low-wavenumber spectral density. Chase (1969) showed that a clamped plate responds $(k_p/k_c)^2$ less than a membrane to the convective peak, where the wavenumbers k_p and k_c refer, respectively, to the wavenumber of the plate and the wavenumber of the convective peak.

In this paper, we discuss the theory of relating plate modal response to the various regions of the turbulent boundary layer, the design of the experiment, and the experimental results.

PLATE MODAL RESPONSE AS A MEASURE OF SPECTRAL DENSITY

The modes of a clamped rectangular plate can be expressed in a product form as a function of x times a function of y. The x dependence of the modes will have either of two forms, depending on whether the mode is spatially even or odd:

$$\psi_1(x) \approx \frac{1}{\sqrt{2}}\left(\cos k_1 x + \sin k_1 \frac{L_1}{2} \frac{\cosh k_1 x}{\sinh k_1 \frac{L_1}{2}}\right) \text{ even} \quad (1a)$$

$$\frac{1}{\sqrt{2}}\left(\sin k_1 x - \cos k_1 \frac{L_1}{2} \frac{\sinh k_1 x}{\cosh k_1 \frac{L_1}{2}}\right), \text{ odd} , \quad (1b)$$

where L_1 is the length of the plate in the x direction, and the determinantal equation for k_1 is given by

$$\tan k_1 \frac{L_1}{2} \pm \tanh \frac{k_1 L_1}{2} = 0 , \quad (2)$$

the upper sign referring to even modes. The expressions for the modal form and the determinantal equation together ensure that

$$\left.\frac{\partial \psi(x)}{\partial x}\right|_{x = \pm \frac{L_1}{2}} = 0 ,$$

and

$$\left.\psi(x)\right|_{x = \pm \frac{L_1}{2}} = 0 .$$

The modes have been approximately normalized by using $\sqrt{2}$ as a constant multiplier. Since all the modes we used experimentally are of high order, this is a reasonable estimate.

The lengths of the sides of the plate were chosen very carefully to separate the frequencies of modes of interest. The wavenumbers k_1 and k_3 satisfy the plate equation,

$$k_1^2 + k_3^2 = \frac{\omega}{\sqrt{\frac{E}{\rho(1-\sigma^2)}}\ \frac{h}{\sqrt{12}}} \quad , \qquad (3)$$

where E is Young's modulus, ρ is density of plate material, σ is Poisson's ratio, and h is the plate thickness. For high order modes, we treat the determinantal equation as the limit in which tanh = 1, which physically corresponds to the effect of the boundary being felt only near the edges of the plate. In this limit, the clamping introduces an extra eighth of a wavelength at each edge, and the determinantal equation takes the simple form

$$k_1^2 + k_3^2 \approx \left[\left(n + \frac{1}{2}\right)\frac{\pi}{L_1}\right]^2 + \left[\left(m + \frac{1}{2}\right)\frac{\pi}{L_3}\right]^2 \quad , \qquad (4)$$

where n and m are the mode numbers in the downstream and cross-stream directions, respectively.

We found, through trial and error, that if the lengths L_1 and L_3 were in the ratio of 3 to 2 there were few modes that had the same frequency as another mode and most modes were reasonably far apart in frequency. For the length ratio of 3 to 2, the determinantal equation becomes

$$\omega \sim k_1^2 + k_3^2 = \frac{\pi^2}{L_1^2 L_3^2}\left\{\left[\left(n + \frac{1}{2}\right)2\right]^2 + \left[\left(m + \frac{1}{2}\right)3\right]^2\right\} . \qquad (5)$$

For n and m on the order of 3 to 10, the number in brackets shows very little redundancy. The locations of solutions to the approximate determinantal equation are shown in Figure 1; note that in this figure the radial distance from the origin is proportional to the square root of the frequency of the mode. We have appended to a number of modes the value of the number in large brackets in Eq. 5, the number being proportional to frequency. During planning of the experiment, we anticipated concentrating on the 7,3 mode having a number 335.25, which leaves it approximately 3% separated in frequency from its nearest neighbor, the 8,2 mode.

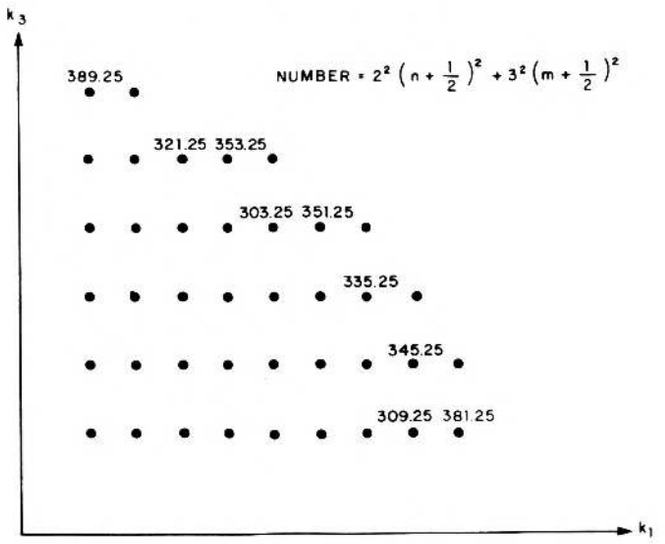

FIGURE 1. MODES OF CLAMPED PLATE WITH SIDES OF 3:2 LENGTH RATIO.

During the experiment, the motion of the plate was sensed with a small accelerometer that was placed on the plate in such a position as to be insensitive to modes antisymmetric in x. Antisymmetric modes curiously have even numbers for their k_1 designation. Thus, the accelerometer is insensitive to the 8,2 mode in particular, along with all other modes antisymmetric in x.

EXPERIMENTAL ARRANGEMENT

The plate, 22.8 in. in diameter, was flush-mounted in a flat surface extending from an open-jet wind tunnel in the manner shown in Figure 2. The active area of the plate is a rectangle of area 500 sq cm with side lengths in the ratio of 3 to 2, the longer side in the downstream direction. The underside of the plate, showing the active area, is illustrated in Figure 3; a side view is given in Figure 4. The outside part was glued to wood to provide mechanical support and damping; large steel bars (1.5 in. × .75 in.) were epoxied to the underside to make a framework defining the active area. The steel bars clamped the plate edge, isolating the active area. The unsupported plate between the wood and the beam, about one quarter the length of a bending wave at frequencies of interest, increased isolation from vibrations of the surrounding

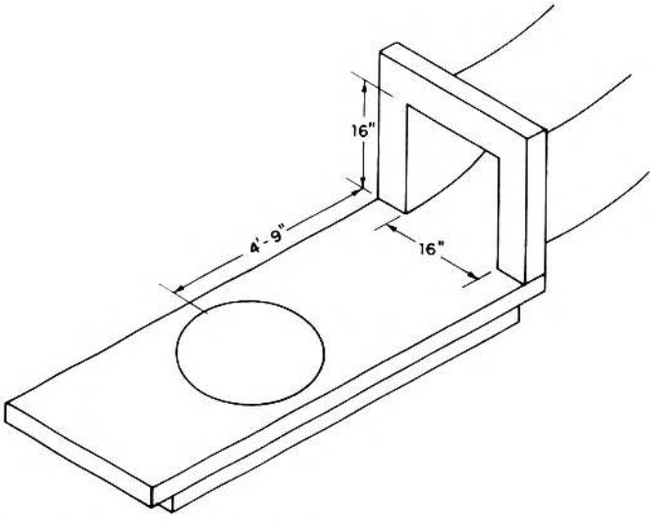

FIGURE 2. EXPERIMENTAL ARRANGEMENT.

surface by acting as a quarter-wave choke. The accelerometer was placed along the midline of the plate at an antinode of a mode having a mode number of 3 across the short side of the plate.

We used the open-jet tunnel, because previous work showed that acoustic noise at the plate, a major experimental contaminant, is greater in ducted flow. Although flow from an open jet is not uniform, it is reasonably so in the vicinity of the plate. The lateral distribution of dynamic pressure at the downstream center of the plate, for typical flow speed, is shown in Figure 5.

Calibration of the Plate

A noncontacting shaker was used to drive the plate, and the resonant frequency and the damping rate of the plate modes were measured. The shaker was a small iron-core magnetic coil placed near, but not touching, the plate. Eddy current repulsion, the force connecting the plate and the coil, was twice the frequency of the current in the coil, the repulsion being a nonlinear effect.

The applied frequency of the driver was swept until a large resonant signal was observed at the accelerometer. We then correlated the frequency of the mode with the predicted value and determined the spatial distribution by using a pencil to map out nodal lines. Nodal lines were mapped at locations where placing the pencil on the plate did not change the response of the accelerometer — i.e., where modal motion was zero and the placing of an object produced no force at the frequency of the mode.

Relation Between Modal Amplitudes and Pressure Spectral Density

The equation of motion of the plate is given by

$$\left(D\nabla^4 + m_p \frac{\partial^2}{\partial t^2} + m_p \beta \frac{\partial}{\partial t}\right) \eta(\vec{x},t) = -p(\vec{x},t) \quad , \qquad (6)$$

where we designate D as the plate stiffness, m_p the mass per unit area, β a loss coefficient, and $\eta(\vec{x},t)$ the displacement of the surface of the plate. We next expand $\eta(\vec{x},t)$ in the normal modes of the plate and the pressure field in its spectral components. Thus,

$$\eta(\vec{x},t) = \sum_{n,m} \psi_{n,m}(\vec{x}) \int_{-\infty}^{+\infty} \frac{d\omega}{2\pi} \eta_{n,m}(\omega) e^{-i\omega t} \qquad (7a)$$

$$p(\vec{x},t) = \int_{-\infty}^{+\infty} \frac{dk_1}{2\pi} \int_{-\infty}^{+\infty} \frac{dk_3}{2\pi} \int_{-\infty}^{+\infty} \frac{d\omega'}{2\pi} p(\vec{k},\omega) e^{i(\vec{k}\cdot\vec{x}-\omega t)} \quad . \qquad (7b)$$

We multiply each side of Eq. 6 by a normal mode shape $\psi_{i,j}(x)$ and integrate over the surface of the plate. It follows that

$$(Dk_{i,j}^4 - m_p\omega^2 - i\omega\beta m_p)\eta_{i,j}(\omega)A_p = - \int_{-\infty}^{+\infty} \frac{dk_1}{2\pi} \int_{-\infty}^{+\infty} \frac{dk_3}{2\pi} S_{i,j}(\vec{k}) p(\vec{k},\omega) \quad , \qquad (8)$$

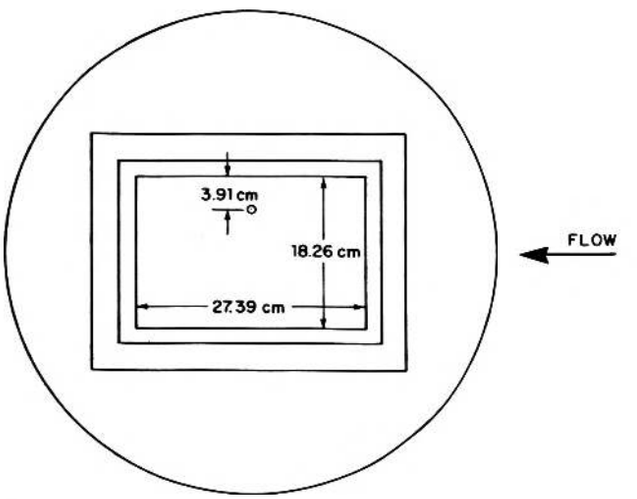

FIGURE 3. UNDERSIDE OF PLATE.

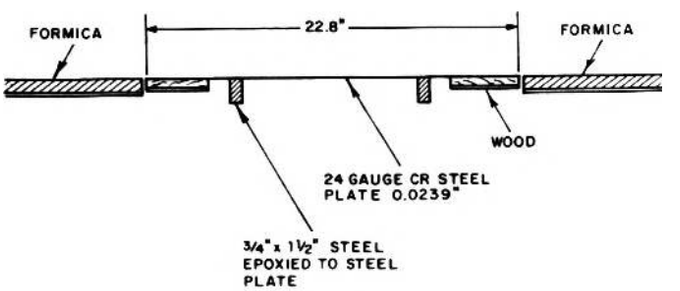

FIGURE 4. SIDE VIEW OF PLATE.

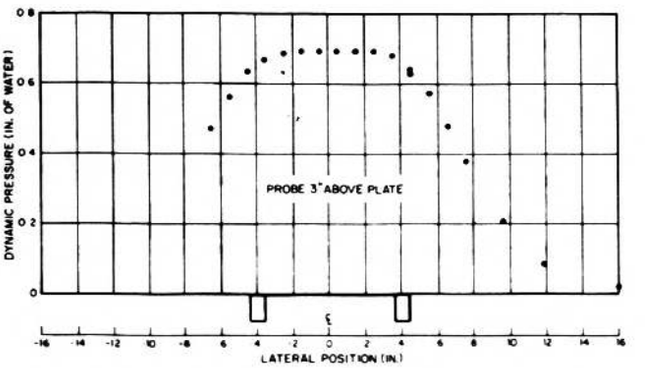

FIGURE 5. LATERAL DISTRIBUTION OF DYNAMIC PRESSURE.

where $S_{i,j}(\vec{k}) = \int d\vec{x}\, e^{i\vec{k}\cdot\vec{x}}\, \psi_{i,j}(\vec{x})$, and A_p is the area of the plate. From this equation, we can solve for $\eta_{i,j}(\omega)$, the amplitude of the i,jth mode.

We next calculate the total time-averaged power $\Pi_{i,j}$ into the i,jth mode of the plate, this power being obtained by multiplying the negative of the instantaneous modal velocity at every point on the plate by the pressure at that point:

$$\Pi_{i,j} = < \int d\vec{x} \left[\frac{-d\eta_{i,j}(t)}{dt}\, \psi_{i,j}(\vec{x}) p(\vec{x},t) \right] >_t \quad , \qquad (9)$$

where $\Pi_{i,j}$ is the average power into the mode and the brackets represent time averaging. By transforming $\eta(t)$ and $p(\vec{x},t)$ and using Eq. 8, we arrive at the intermediate result

$$<\Pi_{i,j}> = - < \int \frac{d\omega'}{2\pi}\, i\omega' \int \frac{d\Omega}{2\pi} \int \frac{d\vec{k}}{(2\pi)^2} \int \frac{d\vec{k}'}{(2\pi)^2} \frac{p(\vec{k},\omega)p^*(\vec{k},\Omega)S(\vec{k})S^*(\vec{k}')}{A_p[Dk^4_{i,j} - \omega^2 m_p - i\omega\beta m_p]} \times e^{i(\vec{k}^*-\vec{k}')-i(\omega-\Omega)t} >_t . \qquad (10)$$

We now invoke the assumption that the pressure spectral components are elements of an ergodic process and that they are independent of each other. Then,

$$<p(\vec{k},\omega)p^*(\vec{k}',\Omega)> = \Phi(\vec{k},\omega)\, \delta\left[\frac{\vec{k}-\vec{k}'}{(2\pi)^2}\right] \delta\left(\frac{\omega-\Omega}{2\pi}\right) \quad . \qquad (11)$$

The integral over frequency is readily performed, because it is an integral over a pole – by assumption very near the axis. The result is

$$<\Pi_{i,j}> = \int_{-\infty}^{+\infty} \frac{d\vec{k}'}{(2\pi)^2} \left[\frac{\Phi(\vec{k}',\omega_{i,j}) + \Phi(\vec{k}',-\omega_{i,j})}{4\, A_p m_p} \right] |S(\vec{k}')|^2 . \qquad (12)$$

This result has a clear physical interpretation. In particular, the power into the mode resonant near $\pm\omega_{i,j}$ accepts energy from the boundary layer in an amount proportional to the square of the overlap function between the mode and the pressure spectral components times the intensity of those components in the boundary layer.

Estimates of the Contribution to $<\Pi_{i,j}>$ From the Convective Peak and From the Low-Wavenumber Region

We first estimate the contribution of the convected peak to the integral. For the case of a perfectly clamped boundary condition the average value of $|S(k_1)|^2$ at values of k_1 near ω/U_c is given by $<|S(k_1)|^2> = \frac{8k^4_{p_1}}{k^6_{1_c}}$ + terms of higher order in k_1/k_{1_c} where $k_{1_c} = \omega/U_c$. This average of S^2 can be obtained by integrating by parts to perform the Fourier transform of the modal response function (Chase, 1969). The integral over k_3 is performed using the dominant modal acceptance in that region. For a convected peak pressure spectral density, we assumed that

$$\Phi(k_{1_c}, k_3, \omega_r) \approx \Phi(\omega_r)\, \frac{\pi}{k_{1_c}} \quad ,$$

where $\Phi(\omega_r)$ is the point pressure spectrum, assumed to be dominated by high wavenumbers. The integral over k_3 is dominated by the major lobe response of the modal overlap function. The convected peak does have energy at low values of k_3, even though it does not at low values of k_1. The total power into a mode from the convected peak is given by

$$\Pi_{n,m(conv)} \approx \Phi(\omega_r)\, \frac{\pi}{k_{1_c}}\, \frac{L_3}{2\, A_p m_p}\, \frac{8k^4_{p_1}}{k^6_{1_c}} \quad . \qquad (13^*)$$

The part of the integral due to the low-wavenumber components is estimated in a simple way. We treat the modal overlap function as if it were that of a large simply supported plate so that the overlap function is sharply peaked at the main lobe. The clamped boundary condition is treated as an end effect that influences the overlap function only at high wavenumbers where end effects are important. Performing these estimates, we arrive at the approximation

$$\Pi_{(low\ k)} = \int_{-\infty}^{+\infty} \frac{dk_1}{2\pi} \int_{-\infty}^{+\infty} \frac{dk_3}{2\pi} \frac{\Phi(\vec{k},\omega_r)|S(\vec{k})|^2}{2\, A_p m_p} \approx \frac{\Phi(k_1,k_3,\omega_r)}{2m_p} \quad . \qquad (14)$$

For these calculations, we have assumed that all functions are double-sided in ω and k. We have assumed that the spectral density in the low-wavenumber region is symmetric in k_1, k_3, and ω.

The experiment was designed with a clamped boundary condition at the edges of the plate so that the convective peak would put a minimum of energy into a plate mode leaving the energy in that mode a good measure of the low wavenumber spectral density in the TBL wall pressure. If the boundary condition at the edge had been a simple support instead of a clamp, the contribution from the convective peak would have been given by the expression,

$$\Pi_{conv} \simeq \Phi(\omega_{i,j}) \frac{\pi}{k_{1_c}} \frac{L_3}{2 A_p m_p} \frac{4 k_{p_1}^2}{k_{1_c}^4} ,$$

which for our typical experimental conditions would have been about 13 dB higher than the result given by Equation 13.

Some estimates have been made for the effect of the less than perfect clamp at the edge of the plate. The rotary inertia of the bars is not infinite so that the moment applied by a mode at the boundary would cause a slight rotation of the bar. The rotary inertia of the bars is so large that the non-zero slope at the edge gives a contribution from the convective peak at least 17 dB smaller than that predicted using equation 13.

The effect of compliance in the epoxy joining the plate and the bar is also a source of a non-zero slope at the edge. Very preliminary estimates suggested that this could be a problem if the epoxy junction were not very stiff. Great care was taken in bonding the bars to the plate to ensure a stiff contact between the two. Small rows of teeth were milled into the contact area of the bars so that when the bars were pressed and epoxied onto the plate there would be significant metal to metal contact between them, thus guaranteeing a stiff contact.

Experimental Technique for Measuring $\langle \Pi_{i,j} \rangle$

We experimentally determine $\langle \Pi_{i,j} \rangle$ by first measuring the energy in a mode with the flow on. Knowing the damping rate, we then know the power dissipated. Since the plate is passive, the power dissipated must be equal to $\langle \Pi_{i,j} \rangle$.

The power dissipated in a mode is equal to the total stored energy in a mode, twice the average kinetic energy, times the time rate of decay of energy. Thus

$$\Pi_{dissipated} = \frac{2 \times 1/2 \, m_p A_p V_{modal}^2}{\tau_e} \qquad (15)$$

where τ_e is the time constant of the energy decay rate, equal to $1/\beta$. Combining with Eq. 14, we deduce that

$$\Phi(k_1, k_3, \omega) \simeq \frac{2 m_p \, 2 \, m_p^2 A_p V_{modal}^2}{\tau_e} \qquad (16)$$

We have reduced our data using this approximation to relate the measured modal velocities and energy decay rate to the low-wavenumber spectral densities.

In using the accelerometer output as a measure of modal response, we corrected for the fact that the accelerometer was at an antinode for 2m + 1,3 modes only and adjusted the assumed value of energy in other modes accordingly. We also made a correction for the mass of the accelerometer loading the plate. In this correction, we approximated the loading by treating the plate as very large so that we could use the point impedance Z_p of an infinite plate. Thus, we assumed that the velocity we would have measured with a massless accelerometer was given by

$$V = \frac{Z_p - i\omega M}{Z_p} V_{meas} \text{ , where M is the accelerometer mass.}$$

Combining this correction with the correction used for determining modal velocity, we have

$$V_{modal} = \left(1 - \frac{iMk_p^2}{8m_p}\right) \frac{V_{meas}(acc)}{\Psi(acc)} ,$$

where $\psi(acc)$ designates the value of the modal shape function at the position of the accelerometer.

EXPERIMENTAL RESULTS

Typical experimental results are shown in Figure 6. Depicted are the rms modal amplitudes of various modes as a function of flow speed over the speed range for which the modal response was not contaminated by acoustic noise, extraneous vibration, or the convected

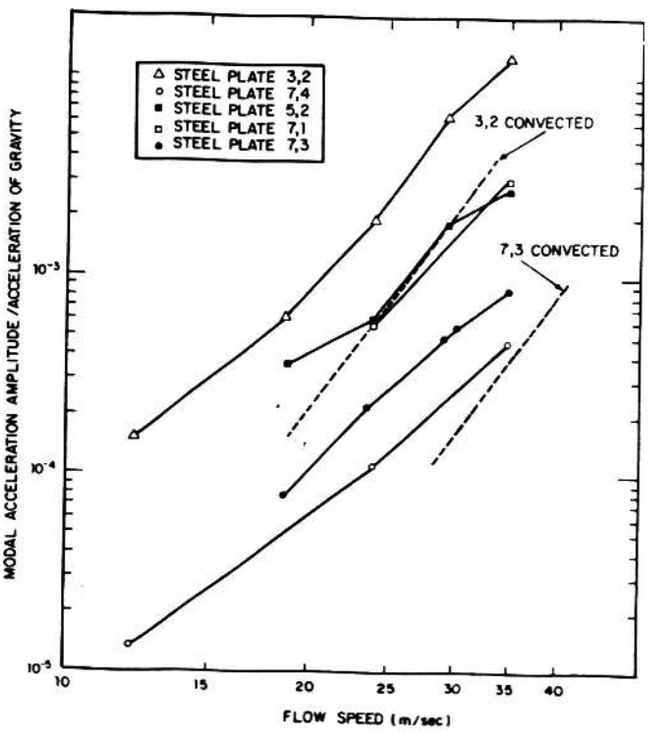

FIGURE 6. TYPICAL EXPERIMENTAL RESULTS

peak. Acoustic noise typically became a problem only at low flow speed, while the convected peak is expected to be a problem only at high speed. Estimates of the contribution of the convected peak to the modal response of the 3,2 and 7,3 modes are also shown in Figure 6.

The level of acoustic contamination was estimated by recording the acoustic pressures in the room with a microphone placed outside the flow. Then, an acoustic source was used to insonify the room and measure the coupling between sound and plate response. From this result, the acoustic contribution to modal excitation was estimated. Only those data were kept for which the acoustic contribution was at least 8 to 10 dB below the other contributors. (We found the effect on modal energies of the vibration of the large wooden platform used to support the plate to be negligible.)

Estimates of the low-wavenumber spectral density, based on measurements with the steel plate, are given in Table I. The deduced spectral densities have been normalized by dividing by the squares of the free-stream dynamic head and the free-stream velocity and multiplying by the cube of the modal resonant frequency in radians.

Experiments were also performed using a brass plate of about the same thickness as the steel. The resonant frequencies for brass were lower. We found more acoustic contamination and, typically, more effects of the convective peak in our results. For these data, we present results only for cases in which the acoustic contamination caused less than about a 2-dB contribution to the measured level; i.e., we corrected our measured modal amplitudes for the acoustic effect, and if the corrected level was closer than 2 dB to the measured level we kept the data. In Table II, we provide the original data (normalized as if there were no contamination), the results with the acoustic contamination subtracted, the calculated contribution from the convected peak, and the corrected result with this latter contribution removed.

Figure 7 presents all the retained data normalized on inner variables v_* and $\omega^+ = (\omega\nu/v_*^2)$, a normalization first proposed and used by Kronauer (1974). The friction velocity was estimated using the formula from Schlicting (1968):

$$\left(\frac{v_*}{U_0}\right)^2 = .0296 \left(\frac{\ell U_0}{\nu}\right)^{-1/5}$$

where ℓ is the distance of the plate center from the nozzle — i.e., 4 ft 9 in.

The boundary layer velocity profile had been measured in a previous series of experiments with virtually the same flow configuration, (Jameson, 1970). It was found in that experiment that the displacement thickness at the location of the plate was almost constant at 0.35 cm for flow speeds over the measured speed range from 9.4 m/sec to 16.5 m/sec. The data in Tables I and II have been plotted in Figure 8 using outer variable normalization assuming that the displacement thickness did remain constant at 0.35 cm

TABLE I. STEEL PLATE DATA.

$$\phi'(7,4) \equiv \frac{\phi(k_{1,7}, k_{3,4}, \omega_{7,4})\omega_{7,4}^3}{q_0^2 U_0^2}$$

U_0 m/sec	$\phi'(3,2)\times10^8$ 487 Hz	$\phi'(5,2)\times10^8$ 830 Hz	$\phi'(7,1)\times10^8$ 1205 Hz	$\phi'(7,2)\times10^8$ 1336 Hz	$\phi'(7,3)\times10^8$ 1612 Hz	$\phi'(7,4)\times10^8$ 1970 Hz
12.3	4.6					0.45
18.0	8.5					
18.1		0.56	1.2		2.2	0.57
18.9	4.6	4.9			1.0	
19.4	11.	0.92	1.5	1.4	1.4	1.9
23.5	46.	3.7	0.03	4.1	4.2	1.3
23.8	13.	3.7	6.6		2.0	0.16
26.9	62.	5.3	2.0	2.8	7.0	0.95
31.7	25.	8.5	16.0		3.1	1.8

TABLE II. BRASS PLATE DATA.

$$\phi'(7,3) \equiv \frac{\phi(k_{1_7}, k_{3_3}, \omega_{7,3})\omega^3_{7,3}}{q_0^2 U_0^2}$$

U_0 m/sec	$\phi'(3,2)\times10^8$ 264 Hz	$\phi'(5,2)\times10^8$ 483 Hz	$\phi'(7,3)\times10^8$ 908 Hz
21.8		16*	↑
		11†	
		(1.9)	
		[9]	
24.1	407*	15*	acoustically contaminated
	300†	9.9†	
	(7.2)	(3.4)	
	[293]	[6.5]	
27.8	538*	50*	
	458†	38†	
	(15)	(6.4)	
	[443]	[32]	
32.6	1870*	176*	
	1667†	157†	
	(28)	(12)	↓
	[1639]	[145]	

* original data
† corrected for acoustic contamination
() estimated convective contribution
[] low-k contribution

over the whole speed range of the experiment. It is to be noted that since δ^* is assumed constant and V_*/U_0 is substantially constant, Figures 7 and 8 are practically identical except for a change in the scales shown on the figures.

ACKNOWLEDGEMENT

The author would like to thank Messrs. Jonathan Spencer and Hugh Wright for assistance with the experimental work and Drs. David Chase and James Barger for continued interest and comment on the experiment. He would also like to thank Mr. Hugh Fitzpatrick of ONR, Code 212, who provided encouragement, advice, and financial support.

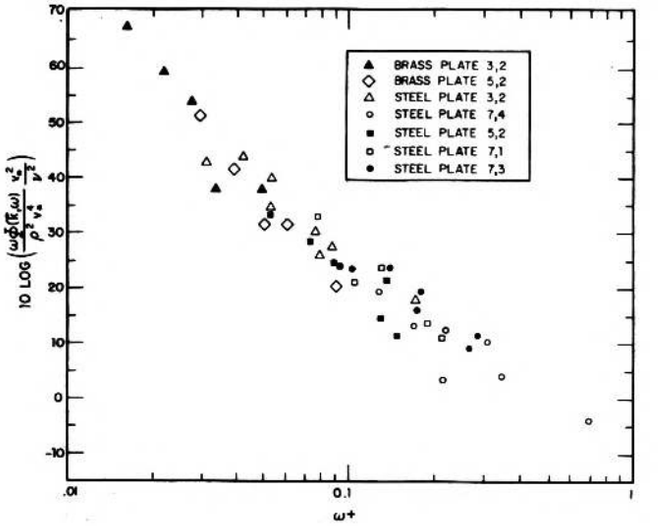

FIGURE 7. NORMALIZED DATA USING INNER VARIABLE SCALING.

REFERENCES

Blake, W.K. and Chase, D.M., 1969, "Wavenumber-Frequency Spectra of Turbulent-Boundary-Layer Pressure Measured by Microphone Arrays", BBN Report No. 1769.

Chase, D.M., 1969, "Turbulent Boundary Layer Fluctuations and Wavenumber Filtering by Nonuniform Spatial Averaging", J. Acoust. Soc. Am., 46, 1350.

Jameson, P.W., 1970, "Measurement of Low-Wavenumber Component of Turbulent Boundary Layer Wall Pressure Spectrum", BBN Report No. 1937.

Kronauer, R., 1974, Personal Communication.

Schlicting, H., 1968, Boundary Layer Theory, 6th Edition, McGraw-Hill Book Company, Inc., New York, Eq. 21.12.

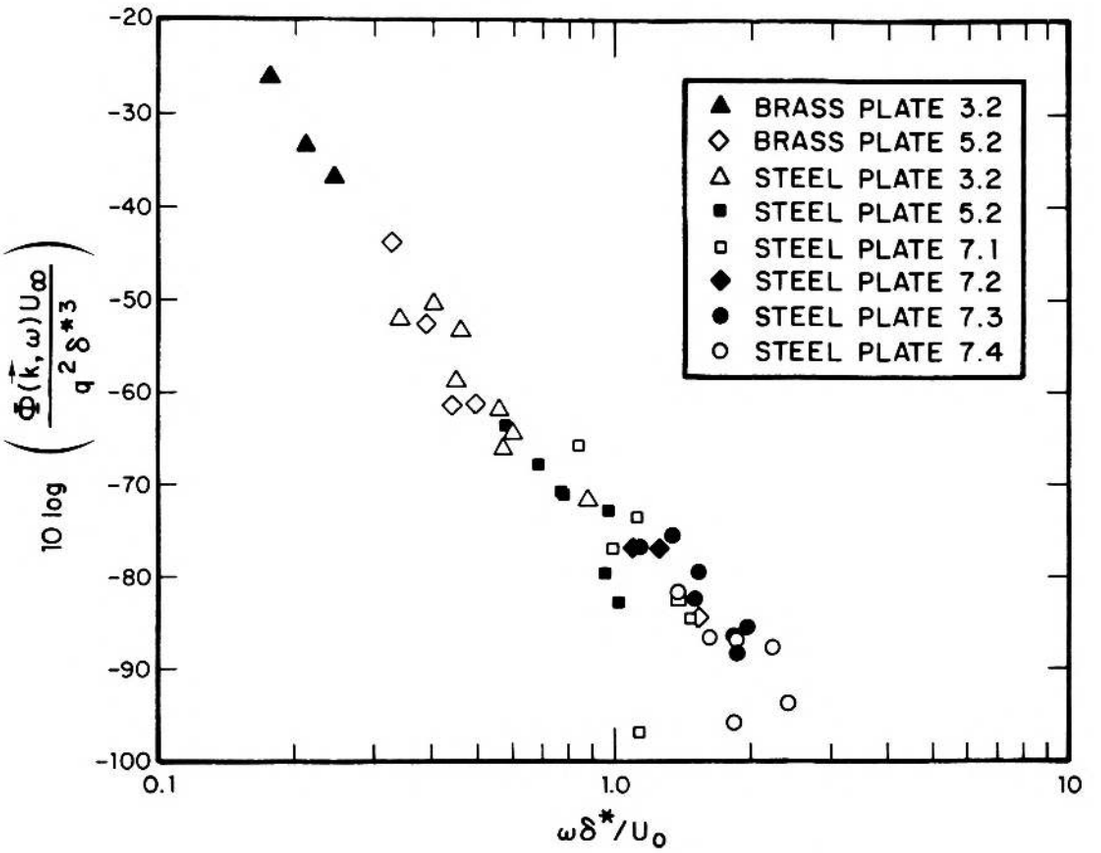

FIGURE 8. NORMALIZED DATA USING OUTER VARIABLE SCALING

DISCUSSION

W. K. Blake, Department of the Navy: Did you measure the actual mode shape of any of the plate modes? Any discontinuity in slope at the edge due to non-ideal clamping would provide more convected wave number response than you estimated.

Jameson: We could not measure this directly. However, qualitatively the response to the pencil was much less sensitive to the pencil near the clamp than near a nodal line. In addition the location of nodal lines out on the plate was consistent with where they would be with a clamp.

J. Laufer, University of Southern California: A couple of questions, could you describe in a little more detail, exactly how the plate is located with respect to the nozzle of the jet? And, how far was your plate measuring station located with respect to the axis of the jet?

Jameson: The nozzle was a 16-inch square nozzle, and the plate was level with the bottom edge of the nozzle. It was 26 inches wide, and the center of the plate was 4 feet, 9 inches downstream from the exit of the nozzle. I would say qualitatively that we pushed the plate as far downstream as we could while staying in the region of flow that was fairly uniform. We wanted to have as thick a boundary layer as we could. So we pushed it down fairly far. We positioned it so that the flow was more or less non-uniform, just beyond the edge of the plate.

Laufer: I'd like to inject a point of caution. Since one is interested in the low wave number excitation produced by the large scale structures, these are considerably different in a jet from those in a boundary layer. Would you not expect the low wave number response would scale not with the sublayer parameters but rather the so-called outer parameters of the boundary layer.

Jameson: I don't really have any strong opinions on what the scaling should be. Scaling on inner variables was Dick Kronauer's suggestion and he has thought about the scaling question much more than I have. I will say parenthetically that there are some other data available taken in water which Jim Barger has looked at and compared with these data and they did scale this way. These data were taken at high values of Ω^+ and fit fairly well. But intuitively, what you're saying sounds right, I would expect it might scale on a larger dimension. (A plot of low wavenumber data using outer variable scaling has been added to the revised paper.)

With respect to the uniformity of the flow, I agree with you it's too bad we couldn't do the test in an entirely uniform flow. But when we did previous tests in a duct we found that it was just a fact that the duct seemed to be just noiser in an acoustic sense. So, in order to get anything we had to get rid of the acoustic noise. We might try this in a much larger flow. We now have a wind tunnel with a considerably larger nozzle, and it might make sense to go there as it is also in a very quiet room.

W. Willmarth, University of Michigan: Could you tell us a little bit more about how you determined that the acoustic inputs and perhaps vibration inputs were not important in the experiment.

Jameson: We measured the ambient acoustic noise in the room and found that most of the noise seemed to come from the edges of the nozzle. We placed a microphone out in the room, outside of the flow so it wasn't affected by the wind but oriented with respect to the nozzle, about the same way that the plate was. We measured the acoustic noise while we were doing the flow experiment. Then we turned on a very large acoustic noise source in the room that was oriented similarly and was located close where the nozzle was and ensonified the room to a very high acoustic level. We measured the response of the plate to that acoustic noise and thereby determined the coupling between vibration of the plate and the acoustic noise of the room. We subtracted that out from our data. We looked at how the acoustic response compared with the total plate response and either subtracted it or only chose those data where that effect was very small. Now, typically for the steel plate the effect was quite small as soon as we got to a flow speed greater than 20 meters per second.

Willmarth: So when you were running with the high speed you didn't have to subtract much of the response.

Jameson: No, we didn't have to subtract. If we had to subtract too much then we threw out the data. And we did have to do that with our brass plates since the brass plates oscillated at lower frequencies and there tended to be more acoustic noise at low frequencies.

Willmarth: How about vibration of the set up, that wasn't caused by acoustics that appeared in the tunnel?

Jameson: There was quite a bit of vibration at the edge of the plate resulting from vortices coming out. What we did there is more or less the same. We went through a very careful vibration isolation job. Basically most of the vibration was coming from where the wooden plate was connected to the nozzle. We put a vibration break in there, a piece of very compliant rubber and we dropped the vibration levels on the wooden plate about 20 db as a result of that. And we noted that the vibration levels on our steel plate didn't change at all. So we concluded that the vibration was not significant.

McConachie: Your measurement sensor, the plate, performs spatial filtering of the flow wave numbers but the accelerometer output contains contributions from all frequencies. An alternative would have been to perform spatial correlations of the filtered signals from two pressure transducers and Fourier transform the results. What is the relative signal to noise advantage of the method presented?

Jameson: I think the spatial response of two pressure transducers has too much response to high wavenumbers. Fourier transforms won't get rid of high wavenumber response of the individual transucers.

R. L. Ash, NASA Langley Research Center: How did the viscous damping shift your "7,3" natural frequency? Damping can have a very significant effect on membrane-like natural frequencies. I wondered how significant were the frequency shifts on clamped plates.

Jameson: We did not observe any change in the Q of the resonance with the flow on or off. We did find a consistent tendency for the resonant frequency to increase slightly with the flow on over what it was with the flow off. Typically,

$f_o \sim 1600$ Hz $U = 0$,
$f_o \sim 1605$ Hz $U = 2000$ cm/sec, and
$Q \sim 2000$.